Extracting Super-resolution Details Directly from a Diffraction-Blurred Image or Part of Its Frequency Spectrum[1]

Edward Y. Sheffield, iLabY
Edward.Y.Sheffield@hotmail.com

Abstract It is usually believed that the low frequency part of a signal's Fourier spectrum represent its profile, while the high frequency part represent its details. Conventional light microscopes filter the high frequency parts of image signals, so that people cannot see the details of the samples (objects being imaged) in the blurred images. However, we find that in a certain condition (*isolated lighting* or named *separated lighting*), a signal's low frequency and high frequency parts not only represent profile and details respectively. Actually, any one of them also contains the full information (including both profile and details) of the sample's structure. Therefore, for samples with spatial frequency beyond diffraction-limit, even if the image's high frequency part is filtered by the microscope, it is still possible to extract the full information from the low frequency part. Based on the above findings, we propose the technique of Deconvolution Super-resolution (DeSu-re), including two methods. One method extract the full information of the sample's structure information directly from the diffraction-blurred image, while the other extract it directly from part of the observed image's spectrum, e.g., low frequency part. Both theoretical analysis and simulation experiment support the above findings, and also verify the effectiveness of the proposed methods.

1. Introduction

In 1873, Ernst Abbe found the diffraction-limit of conventional light microscopes: even the image of an ideal point is an airy-disk-shaped spot rather than an infinitely small point. Therefore, for two points with distance less than a half of the visible light's wavelength, i.e., about 200~300nm, their images overlap with each other and cannot be resolved. Samples' structures smaller than diffraction-limit was unresolvable until super-resolution techniques emerged. These techniques were divided into two categories[1]. The first category use structural-illumination to image the sample several times, and then process the resulting images to get a super-resolution image. Representative techniques: STED[2], RESOLFT[3], SIM[4], NL-SIM[5], et al. The second category manage to turn on individual molecules at different time, i.e., separate them in time, and then also reconstruct a super-resolution image. Representative techniques: STORM[6], PALM[7], PAINT[8], et al. Besides, a technique named MINFLUX[9] combine the advantages of the two categories. It can localize individual molecules with ultra-high precision. There is a different technique named Expansion Microscopy (ExM)[10]. It expand samples physically to resolve structures which are unresolvable directly.

From the point view of Fourier Optic, a sample's ideal image should include all components of spatial frequency, but conventional light microscope filter out all components with frequency higher than a certain cutoff value. As a result, the image observed only include low frequency components, and appears blurred and lacks details. Existing techniques of super-resolution ingeniously transform a sample's high frequency components into low frequency ones, and thereby make them resolvable by light microscopes. For example, in STED, RESOLFT, STORM, PALM and MINFLUX, only part of the sample are turned on each time, and the distances between any two visible points are larger than diffraction-limit. By doing so, the highest spatial frequency of the observed part is decreased. Similarly, SIM illuminated the sample with sinusoidal light pattern. As a result, the high frequency components are shifted into low

[1] Relevant patents have been applied.

PeerJ Preprints | https://doi.org/10.7287/peerj.preprints.27591v1 | CC BY 4.0 Open Access | rec: 16 Mar 2019, publ: 16 Mar 2019

frequency range, and thereby decreased the spatial frequency of the observed sample. Differently, ExM expand the sample physically to decrease its spatial frequency directly. Decreasing samples' spatial frequency equivalently increase the highest frequency detectable by the microscope. Interestingly, similar pre-processing steps may also help human eyes observe tiny structures originally hard to see, and achieve relative "super-resolution". For example, tiny samples could be seen by eyes after physical expansion; dense points turned on separately could be distinguished by eyes; far moiré fringes could be seen by eyes, and then the fine structure could be estimated by its relationship with the moiré fringes.

However, we are still curious about an old question: if a sample's spatial frequency is not decreased, could its detail information passes through a diffraction-limit microscope? Or, if the high frequency components are filtered by the microscope, is there still details included in the structure information extracted from the low frequency components only? The results of this study show that both these are possible, and two methods are proposed to extract the full information in space domain and frequency domain, respectively.

2. Basic knowledge

First of all, an appropriate model should be chosen to represent the images. In this study, we adopt a classic model widely used in the field of Digital Image Processing[11]. The image area is divided into uniform grids, and the light intensity of each grid is represented as a value called pixel value. As a result, the image is represented as a matrix. This matrix (digital image signal) is an approximation of the physical image in given sampling rate and quantization accuracy. The higher the sampling rate, the more the pixels. The higher the quantization accuracy, the more accurate the pixel values. The structure information of samples, which is what people need, is carried in the corresponding digital image signals.

This study is based on a key, but usually ignored phenomenon: information can be carried in the same signal in a variety of ways. There is common opinion in the field of Digital Image Processing: the low frequency part of an image's Fourier spectrum correspond to the sample's profile information, which changes slowly with space; while the high frequency part corresponds to the detail information, which changes fast with space. This opinion is correct for normal imaging system because each pixel value corresponds directly to a grid in image area. Thereby, the spatial structure information is carried directly in pixel values. However, the opinion may not be correct if the information is carried indirectly. Strictly speaking, both high frequency and low frequency components are concepts attached to signals rather than information. They do demonstrate fast-changing or slow-changing forms in space domain. But they may not necessarily correspond to the profile or details of the sample if the information is not carried directly.

Here are some simplified examples about information and its carriers. Example 1: if two physical points are used to carry information, their amount could represent the integer-value "2", or their distance could represent a real-value such as 16.3625940683957262. In this example, the carriers of information are physical objects. In more cases, observed signals are used to carry information. Example 2: in a Single-Molecule-Localization microscope, the observed image of individual molecules is blurred, and the pixel values do not reflect the molecules' spatial structure directly. But people are only interested in the molecules' location information carried in the pixels. It can be extracted, by methods such as data fitting, when the microscope's Point Spread Function (PSF) is known. In both of the examples, prior knowledge plays a key role, and determines how the information is carried in the signals. In example 1, it tells the information needed is carried in the amount or the distance of the two points. In example 2, it provides the template required for data fitting, i.e., the PSF. Besides the above examples, there are some researches[12-14] relevant to how information is carried in signals in complicated or implicit ways.

PeerJ Preprints | https://doi.org/10.7287/peerj.preprints.27591v1 | CC BY 4.0 Open Access | rec: 16 Mar 2019, publ: 16 Mar 2019

We find that in the condition of *isolated lighting*, the observed images always carry the full information of the sample's structure, no matter they are sharp or blurred by diffraction. The pixels of sharp images carry the full information directly, including both profile and details. The blurred images carry only the profile information directly, but carry the full information indirectly. Such a situation of "one carrier, two types of information" is somewhat similar to the above example 1. Different ways of carry lead to different methods for extraction. It is only required to read pixel values directly for the extraction of full information from sharp images. But more complicated procedure is required to extract from blurred images, e.g., solving a system of equations. The basis of this study is the aforementioned image model, no matter for space domain or frequency domain. Therefore, the task of extraction is translated into the calculation of unknown pixel values, or matrix elements. The rough location of the unknown pixels in the image should be estimated first, and this could be done using techniques such as Single-Molecule-Localization. In the following sections, two methods will be described, for space domain and frequency domain respectively.

3. Method for spatial domain

The effect of diffraction to imaging is usually modeled as the convolution of PSF and the ideal images. It diffuses the light intensity of each pixel to other pixels, and thereby lowers the diversity of pixel values, i.e., blurs the images. For convenience, we first explain this procedure on 1D signals. Analogous to the aforementioned image model, a 1D range is also divided into uniform segments, and each segment is represented as one value. Let's take the following simple signal as an example, as shown by Fig. 1. It has two adjacent values which are greater than zero, while all the other values are zeros. This is an analogy to the situation that there are only two point light sources.

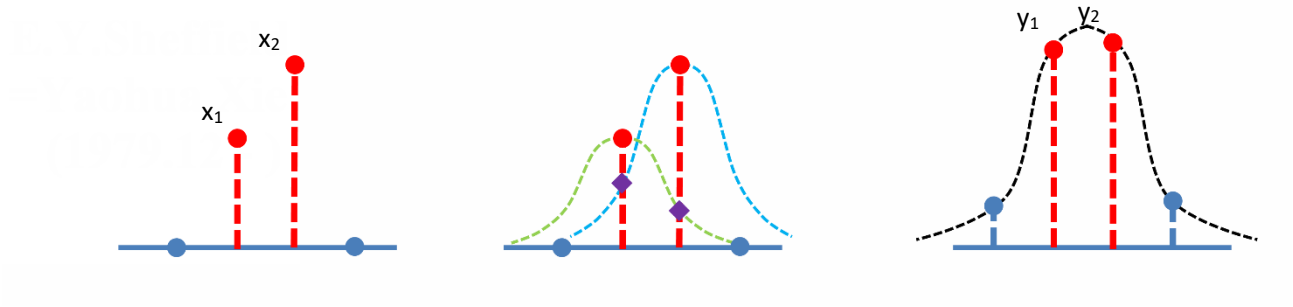

Fig.1. (a) Before convolution (b) During convolution (c) After convolution

Where, Fig. 1(a) shows the 1D signal before convolution, which named "ideal signal" here. The two values in dash line need to be figured out. Fig. 2(b) shows the situation during convolution, where the convolution kernel is known in advance. It is equivalent to the PSF of a 2D imaging system, and called Impulse Response Function (IRF) here. Fig. 1(c) shows the resulting signal after convolution. It is also known in advance, and named "observed signal" here. As the result of convolution, the observed signal looks like the IRF. It is much smoother than the ideal signal, which comprises two impulses. For image signals, being smoother usually means being more blurred, and harder to identify their details.

However, we find that it is possible to recover the ideal signal in a certain sufficient condition, i.e., the condition of isolated lighting (or named separated lighting). This condition means the Region of Interest (ROI) in the sample's image is only affected by its own structure and lighting, and is independent of the rest of the sample and the whole surrounding. For example, only one small area of the sample is lighted, or only one molecule is turned on, while the rest part and the surrounding are either totally dark or have no light collected by the microscope. In practice, an ROI is

PeerJ Preprints | https://doi.org/10.7287/peerj.preprints.27591v1 | CC BY 4.0 Open Access | rec: 16 Mar 2019, publ: 16 Mar 2019

treated to fulfill the condition as long as the effect of the rest part and surrounding is ignorable. For example, all the other light sources are far away from the ROI, and their effect is very slight. The condition of isolated lighting is not difficult to reach in practice. But it provides very strong prior knowledge because it gives infinitely many pixel values outside ROI, i.e., zeros.

For the situation in Fig. 1, the ROI is the locations of the two non-zero values. Isolated lighting means the observed signal's values in the ROI are only relevant to the ideal signal's values in the ROI, and the values of the IRF. The other values of the ideal signal do not affect the result of convolution because they are all zeros. In this case, there is a mathematical relationship among the ideal signal, the IRF and the observed signal. Therefore, the two unknown values in Fig. 1(a) can be figured out from the known IRF and observed signal. Denote:

1. The ideal signal's unknown values are x_1 and x_2 at the left and right, respectively;
2. The amplitude, i.e., the center value of the IRF is p;
3. The IRF has value q_1 at the location of x_1 when its center is at the location of x_2. In Fig. 1(b), the value q_1 is shown by the left dark diamond.
4. The IRF has value q_2 at the location of x_2 when its center is at the location of x_1. In Fig. 1(b), the value q_2 is shown by the right dark diamond.
5. The observed signal has values y_1 and y_2 at the location of x_1 and x_2.

Since the observed signal is the convolution of the ideal signal and the IRF, we get the following system of equations:

$$\begin{cases} y_1 = p \cdot x_1 + q_1 \cdot x_2 \\ y_2 = p \cdot x_2 + q_2 \cdot x_1 \end{cases} \tag{1}$$

The solution of the system of equations is:

$$\begin{cases} x_1 = \frac{p \cdot y_1 - q_1 \cdot y_2}{p^2 - q_1 \cdot q_2} \\ x_2 = \frac{y_1}{q_1} + \frac{p \cdot q_1 \cdot y_2 - p^2 \cdot y_1}{p^2 \cdot q_1 - q_1^2 \cdot q_2} \end{cases} \tag{2}$$

When $p = 1$ and the IRF is symmetrical, i.e., $q_1 = q_2 = q$, formula (2) becomes:

$$\begin{cases} x_1 = \frac{y_1 - q \cdot y_2}{1 - q^2} \\ x_2 = \frac{y_2 - q \cdot y_1}{1 - q^2} \end{cases} \tag{3}$$

For example, suppose that the ideal signal is $(\cdots \quad 1.2 \quad 3.4 \quad \cdots)$, where the suspension points mean infinitely many zeros; the IRF is $(\cdots \quad 0.9981 \quad 1.0 \quad 0.9981 \quad \cdots)$, where the suspension points mean arbitrary values (they do not affect the result in this case); therefore, $p = 1$, $q_1 = q_2 = 0.9981$; the observed signal is $(\cdots \quad 4.5934 \quad 4.5977 \quad \cdots)$, where 4.5934 and 4.5977 are the values of y_1 and y_2 respectively, and suspension points mean the other values. Substitute these values into formula (2) and we get: $x_1 = 1.2$ and $x_2 = 3.4$. In other words, the ideal signal is recovered from the observed signal and the IRF.

It can be seen that only part of the observed signal and the IRF is used. In fact, it is not necessary to y_1 and y_2 which have the corresponding location to x_1 and x_2. The method also works if values at other locations are chosen from the observed signal. In practice, it may be beneficial to relieve the effect of observation errors if more values are used to build an overdetermined system of equations.

Now we will extend the procedure to 2D signals, and describe the situation of imaging, as shown by Fig. 2.

Where, Fig. 2(a) shows the image in ideal conditions, i.e., without the effect of diffraction. The image is named "ideal image" in this case. Fig. 2(b) shows the PSF of the imaging system, which is known in advance. Only the major part of

PeerJ Preprints | https://doi.org/10.7287/peerj.preprints.27591v1 | CC BY 4.0 Open Access | rec: 16 Mar 2019, publ: 16 Mar 2019

the PSF is shown in the figure, and the other part is very far away from the center. Fig. 2(c) shows the image observed by the imaging system, which is named “observed image”. Owing to diffraction, it is the convolution of the ideal image and the PSF.

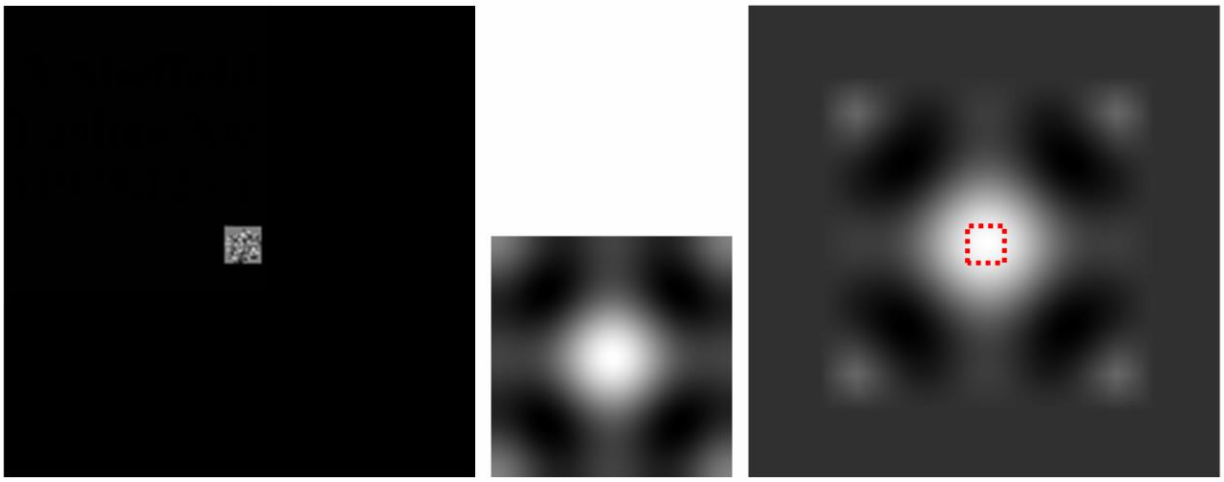

Fig. 2. (a) Before convolution (b) Major part of PSF (c) After convolution

It can be seen that all the pixels in the ideal image equal zeros except in a rectangular ROI. Therefore, the condition of isolated lighting is fulfilled. The PSF’s Fourier spectrum is an ideal low pass filter, and therefore the PSF extends indefinitely in space domain. But its energy or light intensity is strongly concentrated in the center area. The observed image is badly blurred, and looks similar to the PSF. It is very difficult to see any details in the observed image, especially in the ROI, which is shown as a dotted rectangle. In fact, the condition of isolated lighting does not restrict the ROI’s shape. Even an ROI with many disconnected and irregular areas is acceptable, as long as its rough location could be estimated in the observed image. However, one easy way is to find a rectangle to cover all the areas, and then treat the rectangle as the ROI. In order to decrease the complexity of calculation, the rectangle should be as small as possible.

Similar to 1D signals, the observed image’s pixels in the ROI are only relevant to the ideal image’s pixels in the ROI and the PSF. The other pixels in the ideal image do not affect the result of convolution because they are all zeros. In this case, there is a mathematical relationship among the ideal image, the PSF and the observed image. Therefore, the unknown pixels in the ideal image can be figured out from the known PSF and observed image. Let’s:

1. Treat the ideal image’s ROI as an image named $f(k,l)$, $k=1,2,\cdots,M$ and $l=1,2,\cdots,N$; where M and N are the amount of the image’s row and column. k and l start from $(1,1)$ at the image’s most left-top pixel.
2. Denote the PSF as image $p(u,v)$, and set a coordinate with its origin at the PSF’s center. Thereby, the pixel value is $p(0,0)$ at the PSF’s center, and both u and v belong in $[-\infty,+\infty]$;
3. Treat the observed image’s ROI as an image named $g(m,n)$, where $m=1,2,\cdots,M$ and $n=1,2,\cdots,N$.

Let’s take a rotationally symmetrical PSF as an example, and the other PSF could be handled similarly. The observed image is the convolution of the ideal image and the PSF. Specifically, let the PSF overlap the ideal image, and align the PSF’s center with each pixel in the ideal image’s ROI each time. Then, multiply each pixel in the ideal image’s ROI with its corresponding PSF pixel, and accumulate all the results. The accumulative value is the observed image’s pixel value in the corresponding location. The above procedure could be implemented concisely with a program (please refer to

PeerJ Preprints | https://doi.org/10.7287/peerj.preprints.27591v1 | CC BY 4.0 Open Access | rec: 16 Mar 2019, publ: 16 Mar 2019

the source code). In mathematics, this could be expressed with a system of linear equations as follows:

$$Ax = y \tag{4}$$

Where:

$$A = \begin{pmatrix} p(0,0) & \cdots & p(0,N-1) & \cdots & p(M-1,0) & \cdots & p(M-1,N-1) \\ \vdots & \ddots & \vdots & \ddots & \vdots & \ddots & \vdots \\ p(0,-N+1) & \cdots & p(0,0) & \cdots & p(M-1,-N+1) & \cdots & p(M-1,0) \\ \vdots & \ddots & \vdots & \ddots & \vdots & \ddots & \vdots \\ p(-M+1,0) & \cdots & p(-M+1,N-1) & \cdots & p(0,0) & \cdots & p(0,N-1) \\ \vdots & \ddots & \vdots & \ddots & \vdots & \ddots & \vdots \\ p(-M+1,-N+1) & \cdots & p(-M+1,0) & \cdots & p(0,-N+1) & \cdots & p(0,-0) \end{pmatrix}$$

This is a matrix with a size of $(M \cdot N) \times (M \cdot N)$.

$$x = \begin{pmatrix} f(1,1) \\ \vdots \\ f(1,N) \\ \vdots \\ f(M,1) \\ \vdots \\ f(M,N) \end{pmatrix}$$

This is a matrix (vector) with a size of $(M \cdot N) \times 1$, and it is a sequence of all the pixels in the ideal image's ROI, arranged row by row from top to bottom.

$$y = \begin{pmatrix} g(1,1) \\ \vdots \\ g(1,N) \\ \vdots \\ g(M,1) \\ \vdots \\ g(M,N) \end{pmatrix}$$

This is also a matrix (vector) with a size of $(M \cdot N) \times 1$, and it is a sequence of all the pixels in the observed image's ROI, arranged row by row from top to bottom.

The above A is determined by the PSF, and y is determined by the observed image. In other words, both A and y are already known, and x is actually the rearrangement of the ideal image's known pixels. Therefore, the ideal image can be get by solving formula (4). In the above procedure, only the pixels in the observed image's ROI are adopted. Actually, if the other pixels of the observed image are also used, an overdetermined system could be build including more equations. In practice, that may be helpful to improve the method's capability of noise resistance. In this case, the unknowns are still the ideal image's pixels in the ROI because all the other pixels are known to be zeros, in the condition of isolated lighting.

There are many classic or cutting-edge methods could be adopted for solving the above system of equations. Its solvability can be explain as follows. On the one hand, the system of equations should obviously have at least one solution, i.e., the ideal image itself. On the other hand, the PSF is physically the image of an ideal point, and thereby its light intensity should be no smaller than zero at any location. In the model described in section 2, the PSF should be a 2D image signal (matrix) with no values (elements) smaller than zeros. Furthermore, the PSF would be much larger than the ROI when the zooming factor is large enough. As a result, only the center part of the PSF (the Airy disk) affects the convolution results within the ROI. The other part of the PSF would affect the convolution results outside the ROI. For super-resolution microscope, the values of the PSF's center part could be treated as always greater than

PeerJ Preprints | https://doi.org/10.7287/peerj.preprints.27591v1 | CC BY 4.0 Open Access | rec: 16 Mar 2019, publ: 16 Mar 2019

zeros. Therefore, the elements of matrix A are all positive. In addition, the elements of vector x are all non-negative also, thereby $Ax = 0$ is true only when $x = 0$. In other words, the system of homogeneous linear equations $Ax = 0$ only has the zero solution. According to the property of a system of linear equations, the corresponding system of nonhomogeneous linear equations $Ax = y$ has only one solution[15] (i.e., the ideal image).

In the above procedure, the ideal image is figured out by building and solving a system of equations. This seems to be unreasonable in frequency domain because the high frequency part of the image signal cannot pass through the imaging system at all. However, we find that the full information of the sample's spatial structure could be recovered even with only a small amount of low frequency elements. In the following section, we will describe another method which figures out all the ideal image's pixels in the ROI with low frequency elements.

4. Method for frequency domain

The convolution caused by diffraction is equivalent to filtering the ideal image with a low pass filter. Assume that the ideal low pass filter's amplitude is 1, without loss of generality. First, let describe the method on a 1D signal, as shown by Fig. 3.

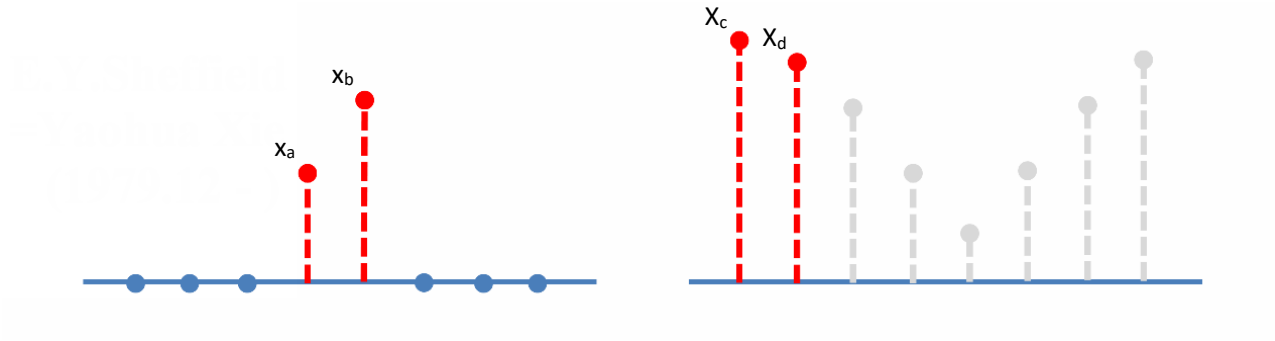

Fig. 3. (a) The ideal signal (b) The corresponding spectrum

Where, Fig. 3(a) shows the ideal signal. It has only two unknown value which are adjacent, while all the other values are zeros. Therefore, the condition of isolated lighting is fulfilled. Fig. 3(b) shows the ideal signal's Fourier spectrum. After low pass filtering, all the high frequency components are removed. Therefore, the known spectrum only includes low frequency components, and is named "observed spectrum" here. For example, the most left two values in the spectrum are preserved, and treated as the observed spectrum. The low pass filter is equivalent to the IRF's Fourier spectrum, which is named System Transfer Function (STF) here. In this case, there is a mathematical relationship among the ideal signal and the observed spectrum. Assume that:

1. The length of the ideal signal is N, and $N \geq 2$;
2. The ideal signal's unknown values are x_a and x_b respectively, where both a and b are integers within $[0, N-1]$;
3. Arbitrarily choose two values X_c and X_d from the observed spectrum, where both c and d are integers.

For the following formula of 1D discrete Fourier Transform[16]:

$$X_k = \sum_{n=0}^{N-1} x_n \cdot e^{-\frac{2\pi i}{N} k \cdot n} \tag{5}$$

Since all the ideal signal's values are zeros except x_a and x_b, the above spectrum becomes:

$$X_k = x_a \cdot e^{-\frac{2\pi a k i}{N}} + x_b \cdot e^{-\frac{2\pi b k i}{N}} \tag{6}$$

PeerJ Preprints | https://doi.org/10.7287/peerj.preprints.27591v1 | CC BY 4.0 Open Access | rec: 16 Mar 2019, publ: 16 Mar 2019

Let k equals c and d respectively, then substitute them into formula (6), and we get:

$$\begin{cases} X_c = x_a \cdot e^{-\frac{2\pi aci}{N}} + x_b \cdot e^{-\frac{2\pi bci}{N}} \\ X_d = x_a \cdot e^{-\frac{2\pi adi}{N}} + x_b \cdot e^{-\frac{2\pi bdi}{N}} \end{cases} \tag{7}$$

Solve the above system of linear equations, and we get:

$$x_a = \frac{X_c \cdot e^{\frac{-2\pi bdi}{N}} - X_d \cdot e^{\frac{-2\pi bci}{N}}}{e^{\frac{-2\pi(ac+bd)i}{N}} - e^{\frac{-2\pi(ad+bc)i}{N}}} \tag{8}$$

And:

$$x_b = \frac{X_c - x_a \cdot e^{\frac{-2\pi aci}{N}}}{e^{\frac{-2\pi bci}{N}}} \tag{9}$$

For example, assume that the ideal signal is $(0 \quad 0 \quad 0 \quad 6.7 \quad 8.9 \quad 0 \quad 0 \quad 0)$, and the corresponding Fourier spectrum is $(15.6 \quad -13.6376 - 4.7376i \quad \cdots)$. In the latter, the complex numbers 15.6 and $-13.6376 - 4.7376i$ are the low frequency components of the observed spectrum, and the suspension points represent the other components. Therefore, $N = 8$, $a = 3$, $b = 4$, $c = 0$, $d = 1$, $X_c = 15.6$, $X_d = -13.6376 - 4.7376i$. Please note that a, b, c, d are all coordinate values of 1D signals, which start from 0. Substitute the above values into formulas (8) and (9), and we get $x_a = 6.7$ and $x_b = 8.9$. In other words, the ideal signal is recovered from the observed (low frequency) spectrum.

It can be seen that only two frequency components of the observed spectrum are used. Actually, they could be chosen from the low frequency part, or the high frequency part, or even arbitrary part. This method works as long as a system of equations is built and a unique solution is got. In practice, it may be beneficial to relieve the effect of errors if more frequency components are used to build an overdetermined system of equations.

Now we will extend the procedure to 2D signals, and describe the situation of imaging. In this case, the IRF is called Optical Transfer Function (OTF) which is equivalent to the PSF's Fourier spectrum, as shown by Fig. 4.

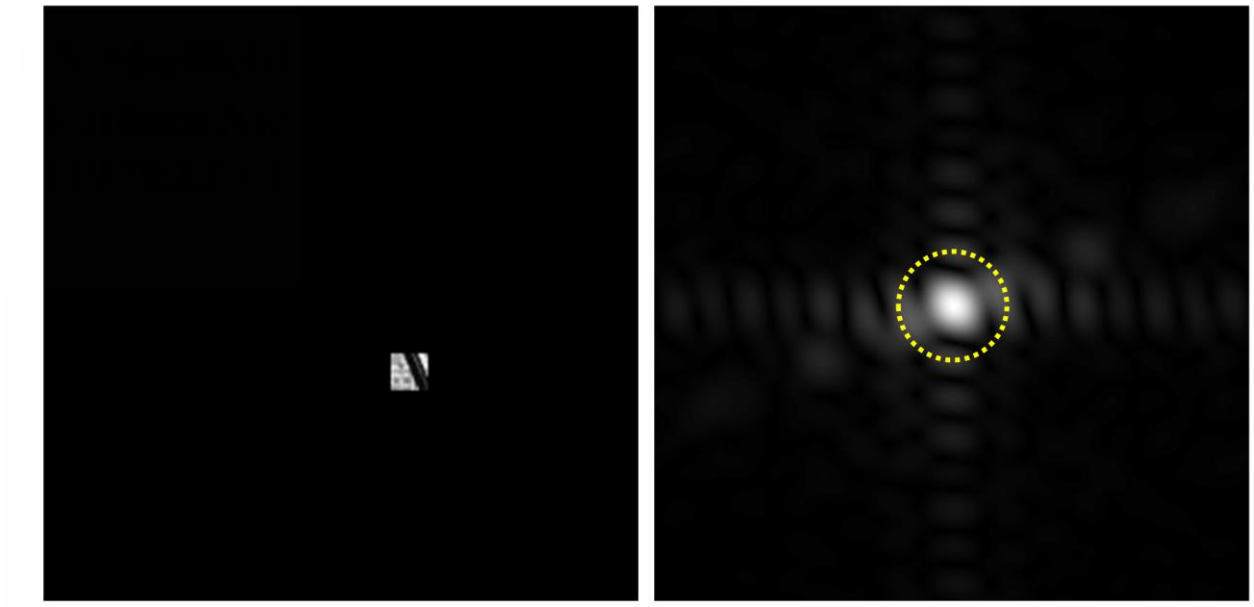

Fig. 4. (a) The ideal image (b) The corresponding spectrum

PeerJ Preprints | https://doi.org/10.7287/peerj.preprints.27591v1 | CC BY 4.0 Open Access | rec: 16 Mar 2019, publ: 16 Mar 2019

Where, Fig. 4(a) shows the ideal result without being filtered, which is named “ideal image”. Fig. 4(b) shows the ideal image’s spectrum of 2D discrete Fourier transform. After being filtered by a low pass filter, the spectrum’s components outside the dotted circle are all removed. Thereby, the known spectrum includes components inside the circle only, and is named “observed spectrum”. Please note that the low frequency components are shown in the center of Fig. 4(b) conventionally. But the spectrum is still in original format in the following procedure, i.e., the high frequency components are in the center. In this case, the condition of isolated lighting is fulfilled, so there is a mathematical relationship between the ideal image and the observed spectrum. Assume that:

1. The ideal image is $x(m,n)$, where $m=1,2,\cdots,M$， $n=1,2,\cdots,N$, and M and N are the amount of the image’s row and column; m and n start from $(1,1)$ at the image’s most left-top pixel;
2. The size of the ideal image’s ROI is $K\times L$, and the row number and the column number of the ROI’s left-top pixel are a and b, respectively;
3. The ideal image’s full spectrum is $Y(u,v)$, where $u=1,2,\cdots,M$， $v=1,2,\cdots,N$;
4. Choose a rectangular area from the observed spectrum, with a size of $K\times L$; the row number and the column number of its left-top pixel are c and d, respectively; for example, $c=d=0$.

For the following formula of 2D discrete Fourier transform[11]:

$$Y(u,v)=\frac{1}{MN}\cdot\sum_{m=0}^{M-1}\sum_{n=0}^{N-1}x(m,n)\cdot e^{-2\pi i\left(\frac{m\cdot u}{M}+\frac{n\cdot v}{N}\right)} \tag{10}$$

Since all the ideal image's pixels are zeros except those within the ROI, the above spectrum becomes:

$$Y(u,v)=\frac{1}{MN}\cdot\sum_{m=a}^{a+K-1}\sum_{n=b}^{b+L-1}x(m,n)\cdot e^{-2\pi i\left(\frac{m\cdot u}{M}+\frac{n\cdot v}{N}\right)} \tag{11}$$

Substitute the chosen components of the observed spectrum into formula (11), and we get a system of equations $Ax=y$, where :

$$A=\frac{1}{MN}\cdot\begin{pmatrix} e^{-2\pi i\left(\frac{a\cdot c}{M}+\frac{b\cdot d}{N}\right)} & \cdots & e^{-2\pi i\left(\frac{a\cdot c}{M}+\frac{(b+L-1)\cdot d}{N}\right)} & \cdots & e^{-2\pi i\left(\frac{(a+K-1)\cdot c}{M}+\frac{b\cdot d}{N}\right)} & \cdots & e^{-2\pi i\left(\frac{(a+K-1)\cdot c}{M}+\frac{(b+L-1)\cdot d}{N}\right)} \\ \vdots & \ddots & \vdots & \ddots & \vdots & \ddots & \vdots \\ e^{-2\pi i\left(\frac{a\cdot c}{M}+\frac{b\cdot(d+L-1)}{N}\right)} & \cdots & e^{-2\pi i\left(\frac{a\cdot c}{M}+\frac{(b+L-1)\cdot(d+L-1)}{N}\right)} & \cdots & e^{-2\pi i\left(\frac{(a+K-1)\cdot c}{M}+\frac{b\cdot(d+L-1)}{N}\right)} & \cdots & e^{-2\pi i\left(\frac{(a+K-1)\cdot c}{M}+\frac{(b+L-1)\cdot(d+L-1)}{N}\right)} \\ \vdots & \ddots & \vdots & \ddots & \vdots & \ddots & \vdots \\ e^{-2\pi i\left(\frac{a\cdot(c+K-1)}{M}+\frac{b\cdot d}{N}\right)} & \cdots & e^{-2\pi i\left(\frac{a\cdot(c+K-1)}{M}+\frac{(b+L-1)\cdot d}{N}\right)} & \cdots & e^{-2\pi i\left(\frac{(a+K-1)\cdot(c+K-1)}{M}+\frac{b\cdot d}{N}\right)} & \cdots & e^{-2\pi i\left(\frac{(a+K-1)\cdot(c+K-1)}{M}+\frac{(b+L-1)\cdot d}{N}\right)} \\ \vdots & \ddots & \vdots & \ddots & \vdots & \ddots & \vdots \\ e^{-2\pi i\left(\frac{a\cdot(c+K-1)}{M}+\frac{b\cdot(d+L-1)}{N}\right)} & \cdots & e^{-2\pi i\left(\frac{a\cdot(c+K-1)}{M}+\frac{(b+L-1)\cdot(d+L-1)}{N}\right)} & \cdots & e^{-2\pi i\left(\frac{(a+K-1)\cdot(c+K-1)}{M}+\frac{b\cdot(d+L-1)}{N}\right)} & \cdots & e^{-2\pi i\left(\frac{(a+K-1)\cdot(c+K-1)}{M}+\frac{(b+L-1)\cdot(d+L-1)}{N}\right)} \end{pmatrix}$$

This is a matrix with a size of $(K\cdot L)\times(K\cdot L)$.

$$x=\begin{pmatrix} x(a,b) \\ \vdots \\ x(a,b+L-1) \\ \vdots \\ x(a+K-1,b) \\ \vdots \\ x(a+K-1,b+L-1) \end{pmatrix}$$

This is a matrix (vector) with a size of $(K\cdot L)\times 1$, and it is a sequence of all the pixels in the ideal image’s ROI, arranged row by row from top to bottom.

PeerJ Preprints | https://doi.org/10.7287/peerj.preprints.27591v1 | CC BY 4.0 Open Access | rec: 16 Mar 2019, publ: 16 Mar 2019

$$y = \begin{pmatrix} y(c,d) \\ \vdots \\ y(c,d+L-1) \\ \vdots \\ y(c+K-1,d) \\ \vdots \\ y(c+K-1,d+L-1) \end{pmatrix}$$

This is also a matrix (vector) with a size of $(K \cdot L) \times 1$, and it is a sequence of the chosen components of the observed spectrum, arranged row by row from top to bottom.

Similar to the method for spatial domain, vector x can be got by solving $Ax = y$, and the ideal image can be got by the rearrangement of x. Although the rectangular area are chosen from the observed spectrum, other shapes or even randomly chosen components are also allowed in this method. This method works as long as a system of equations is built and a unique solution is got. In practice, it may be beneficial to relieve the effect of errors if more frequency components are used to build an overdetermined system of equations.

It can be seen that larger ROI could be recovered if more spectrum components are preserved after filtering. In an extreme case, the ROI is as large as the ideal image. Since all the spectrum components are known, the ideal image could be got directly with inverse Fourier transform or inverse filtering. Actually, it is a classic way recovering a full image from its full Fourier spectrum. This study find another possibility: recovering a ROI image, with full details, from part of its Fourier spectrum (could include only low frequency). That means even low frequency components carry full details of a sample's spatial structure, and seems inconsistent with usual opinions. After excluding several explanations, we believe that the reason is the "integrity of spectrum", i.e., different frequency components are tightly related. Let's take 2D case as an example. As can be seen from the formula of 2D discrete Fourier transform, the spectrum is actually the accumulation of the products of each pixel $x(m,n)$ with its corresponding basis function in frequency domain. Each product is as follows:

$$\frac{1}{MN} \cdot x(m,n) \cdot e^{-2\pi i\left(\frac{m \cdot u}{M} + \frac{n \cdot v}{N}\right)}$$

This is a function includes all frequency components, and its amplitude is affected by the corresponding pixel value $x(m,n)$. When the pixel value varies, the function's value at any frequency changes accordingly with the same percentage. In other words, each pixel value is carried on the amplitude of its corresponding function, and the function's value at each frequency carries its corresponding pixel value. Taking an extreme situation as an example, there is only one function (product) in the image's spectrum when there is only one pixel in the image. In other words, the spectrum is the products of the only pixel with its corresponding basis function. When M, N and the pixel's location (m,n) is known, the basis function $\frac{1}{MN} \cdot e^{-2\pi i\left(\frac{m \cdot u}{M} + \frac{n \cdot v}{N}\right)}$ is also known. Therefore, extract the observed spectrum's value at any frequency and then divided it by the basis function's value at the same frequency, and the result is the unknown pixel value $x(m,n)$. Actually, the frequency could be zero frequency, i.e., DC component in this case. This situation is similar to that when individual molecule's light intensity is extracted by the technique of Single-Molecule-Localization. For the situation of more than one unknown pixels, they could be figured out by building and solving a system of equations, as shown by the aforementioned procedure. It can be seen that when the ROI is smaller than the ideal image, the full spectrum is relatively redundant, and not all components are necessary for the recovery of the ideal image. Blurred images without high frequency components looks meaningless and less

PeerJ Preprints | https://doi.org/10.7287/peerj.preprints.27591v1 | CC BY 4.0 Open Access | rec: 16 Mar 2019, publ: 16 Mar 2019

informative, but they actually contains the full information of the ideal image, in the condition of isolated lighting. In other words, after different ideal images are filtered, the resulting blurred images seem all the same. But they are actually different from one another, as can be seen from formula (10). From the information theory point of view, that means they are distinguishable, and carry different information. This is the foundation of recovery.

Besides, please note that the results of ideal low pass filtering extend indefinitely in spatial domain, no matter for 1D or 2D situation. Therefore, in order to get the accurate spectrum by Fourier transform, all the observed signal (or at least sufficient signal, in practice) should be collected in the indefinitely extended spatial domain.

4. Simulation experiments[2]

Simulation experiments are performed for spatial domain and frequency domain respectively. Each ideal image tested are of size 256×256, and has a ROI in it. Then, 19 different sizes of ROI, i.e., 2×2, 3×3, $\cdots$, 20×20 pixels, are tested for both spatial domain and frequency domain respectively. Furthermore, 20 random tests are performed for each size. The pixel values in the ROI are randomly generated in each test. Therefore, $19 \times 20 = 380$ ideal images are tested for spatial domain and frequency domain, respectively.

a) Experiment for spatial domain

In theory, the Airy-shaped PSF extends indefinitely. But according to the analysis in section 3, the convolution result in the ROI is affected only by the PSF's center area when the PSF is large enough. Therefore, the PSF of size 161×161 is adopted in this experiment, and its major part is shown by Fig. 5(a). The PSF's Fourier spectrum is shown by Fig. 5(b), which is an ideal low pass filter. All the components are removed if they are more distant than 2 pixels to the center.

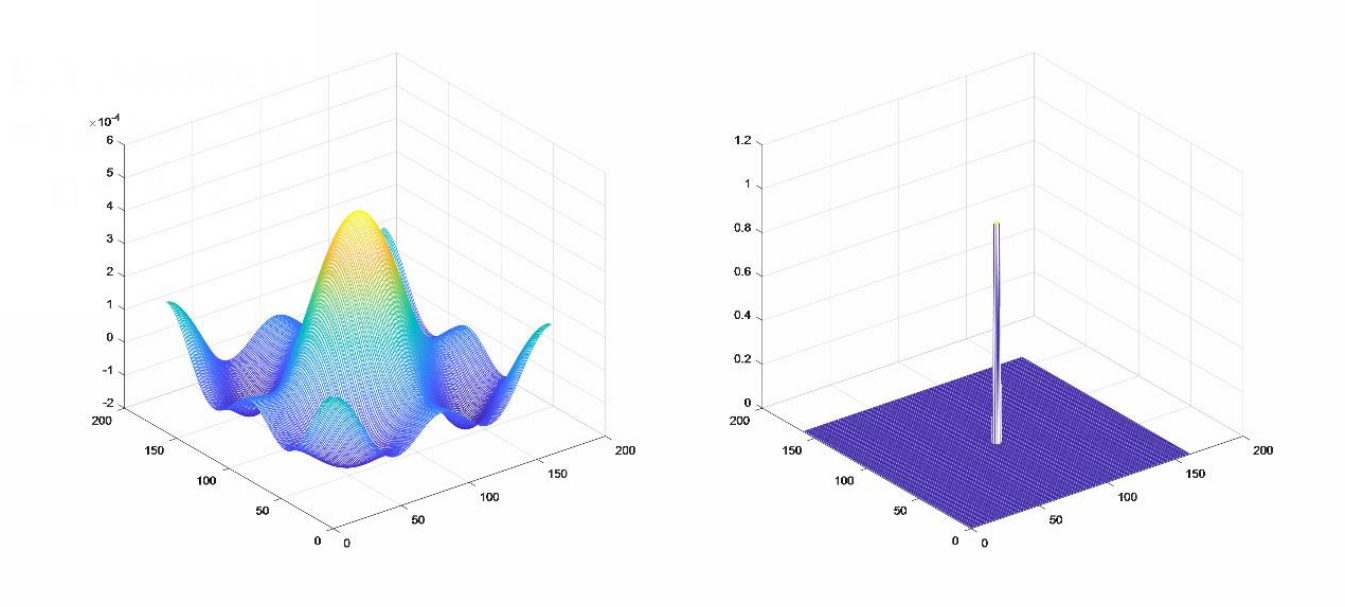

Fig. 5. (a) The major part of the PSF (b) The PSF's Fourier spectrum

After convolution, all the observed images look like Fig. 2(c), but they actually carry different information. Figure out the ideal images' unknown pixels using the method for spatial domain, and the averaged errors of the results are shown by Fig. 6.

[2] Matlab code and test data are released with this paper.

PeerJ Preprints | https://doi.org/10.7287/peerj.preprints.27591v1 | CC BY 4.0 Open Access | rec: 16 Mar 2019, publ: 16 Mar 2019

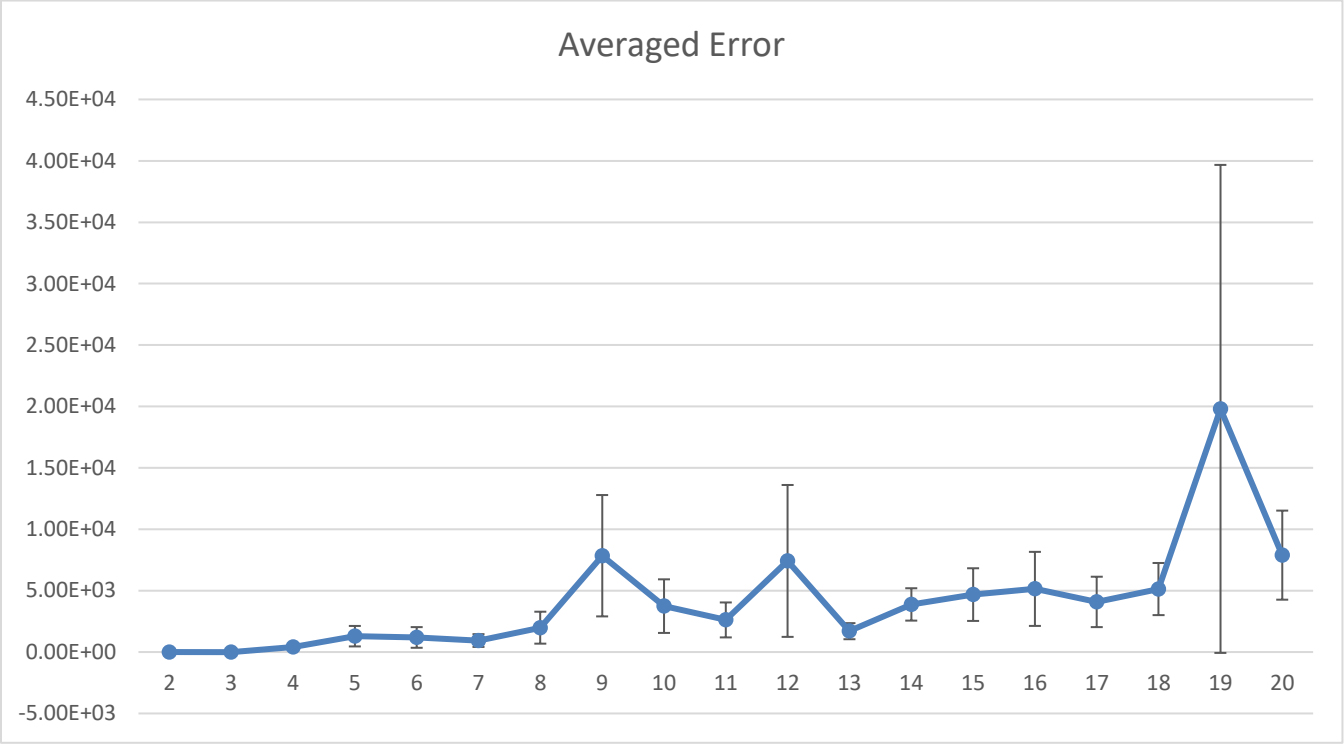

Fig. 6. The averaged errors for the spatial domain method

Where, lateral axis shows the ROI's size, from 2×2 to 20×20 pixels. Vertical axis shows the averaged error, which means the average of all the 20 testing errors for each size. The testing error is defined as: $\|x - x'\|/(K \cdot L)$, which represents the mean square error between the recovered pixels and their corresponding pixels in the ideal image. In the formula, x' represents the vector rearranged from the ideal image's pixels in the ROI. All the averaged errors are also shown in Table 1, where 6.0E-08 means 6.0×10^{-8}, and the rest may be deduced by analogy.

Table 1. The Averaged Errors (AE) for the spatial domain method

ROI size		2×2	3×3	4×4	5×5	6×6	7×7	8×8	9×9	10×10
AE		6.0E-08	0.48	404.76	1293.20	1189.80	938.46	1984.92	7845.30	3739.94
ROI size	11×11	12×12	13×13	14×14	15×15	16×16	17×17	18×18	19×19	20×20
AE	2615.29	7420.87	1699.39	3879.09	4679.25	5144.12	4082.38	5130.22	19800.53	7891.91

It can be seen from Table 1 that the averaged errors are very tiny for size 2×2 and 3×3. Given the maximal pixel value is 256, the recovered results could be treated as almost the same to the corresponding ideal images. That verifies the effectiveness of the method: the spatial resolution is increased by 3 times in each dimension if an individual pixel is resolved into 3×3 pixels with full details. For size 4×4 to 20×20, the averaged errors are larger, and it is hard to judge whether the method still works in these cases. Therefore, we substitute the vector of ideal image, i.e., x' into formula (4), and then calculate the difference value $\|Ax' - y\|/(K \cdot L)$. By checking the difference value, we can see whether the ideal images fulfill the corresponding system of equations. For each size of ROI, the difference values are averaged for all the 20 random tests. The results are named Averaged Differences (ADs), as shown in Table 2.

PeerJ Preprints | https://doi.org/10.7287/peerj.preprints.27591v1 | CC BY 4.0 Open Access | rec: 16 Mar 2019, publ: 16 Mar 2019

Table 2. The Averaged Differences (ADs) for the spatial domain method

ROI size		2×2	3×3	4×4	5×5	6×6	7×7	8×8	9×9	10×10
AD		1.77E-17	2.29E-17	4.01E-17	5.17E-17	8.11E-17	1.06E-16	1.18E-16	1.90E-16	2.10E-16
ROI size	11×11	12×12	13×13	14×14	15×15	16×16	17×17	18×18	19×19	20×20
AD	2.19E-16	3.05E-16	3.82E-16	4.06E-16	4.20E-16	4.32E-16	5.57E-16	6.86E-16	7.56E-16	7.97E-16

In addition, the standard deviations of difference values are less than $1\mathrm{E}-16$ for all the above sizes. According to these results, the system of equations $Ax=y$ can model the imaging procedure accurately enough. That suggests that the large errors in Table 1 are not caused by the method's principle. More accurate results could be got if more effective approaches are used to solve the system of equations, and this could be done in future studies. Therefore, the method's effectiveness is also supported indirectly for size 4×4 to 20×20. In principle, this method could achieve unlimited resolutions.

b) Experiment for frequency domain

In this experiment, the observed image's frequency spectrum is unknown except its low frequency part. Figure out the ideal image's unknown pixels using the method described in section 4, and the resulting averaged errors are as shown in Fig. 7.

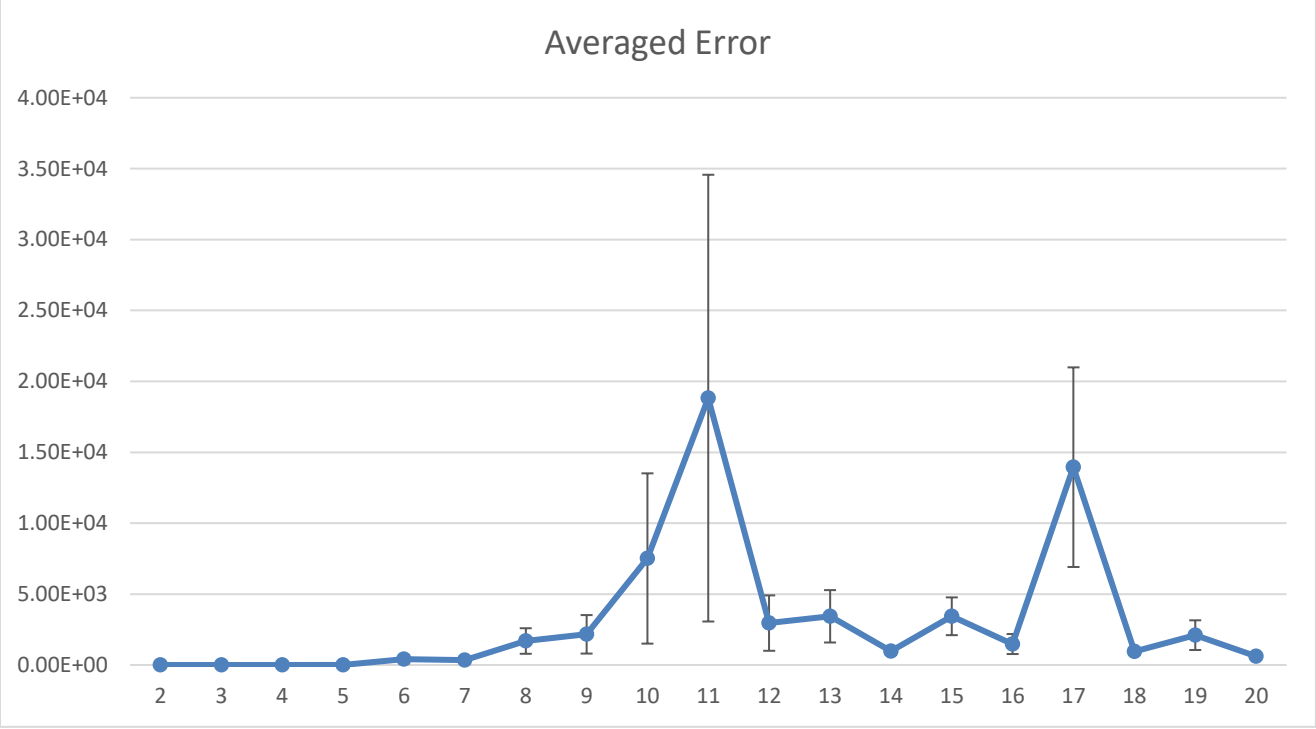

Fig. 7. The averaged errors for the frequency domain method

Similar to the experiment for spatial domain, the lateral axis shows the ROI's size, and the vertical axis shows the averaged errors. All the averaged errors are also shown in Table 3.

Table 3. The Averaged Errors (AE) for the frequency domain method

ROI size		2×2	3×3	4×4	5×5	6×6	7×7	8×8	9×9	10×10
AE		1.24E-10	1.76E-06	6.36E-04	0.38	411.37	335.59	1691.29	2162.04	7510.42

PeerJ Preprints | https://doi.org/10.7287/peerj.preprints.27591v1 | CC BY 4.0 Open Access | rec: 16 Mar 2019, publ: 16 Mar 2019

ROI size	11 × 11	12 × 12	13 × 13	14 × 14	15 × 15	16 × 16	17 × 17	18 × 18	19 × 19	20 × 20
AE	2615.29	18817.96	2954.93	3433.45	983.49	3435.12	1477.80	13948.69	959.28	2103.89

As can be seen from Table 3, the averaged errors are very tiny for size 2×2 to 5×5. Therefore, the recovered results could be treated as almost the same to the corresponding ideal images. That verifies the effectiveness of the method: the spatial resolution is increased by 5 times in each dimension if an individual pixel is resolved into 5×5 pixels with full details. For size 6×6 to 20×20, the Averaged Differences (ADs) are also calculated as shown by Table 4.

Table 4. The Averaged Differences (ADs) for the frequency domain method

ROI size		2 × 2	3 × 3	4 × 4	5 × 5	6 × 6	7 × 7	8 × 8	9 × 9	10 × 10
AD		8.77E-14	1.57E-13	2.26E-13	3.50E-13	5.04E-13	7.01E-13	8.80E-13	1.08E-12	1.26E-12
ROI size	11 × 11	12 × 12	13 × 13	14 × 14	15 × 15	16 × 16	17 × 17	18 × 18	19 × 19	20 × 20
AD	1.40E-12	1.65E-12	1.68E-12	1.62E-12	1.54E-12	1.47E-12	1.35E-12	1.31E-12	1.27E-12	1.29E-12

In addition, the standard deviations of difference values are less than $1\mathrm{E}-12$ for all the above sizes. According to these results, the system of equations $Ax = y$ can model the imaging procedure accurately enough. More accurate results could be got if more effective approaches are used to solve the system of equations, and this could be done in future studies. Therefore, the method's effectiveness is also supported indirectly for size 6×6 to 20×20.

6. Conclusion

In the field of Information Technology, it is usually believed that low frequency spectrums correspond to profile information, while high frequency spectrums correspond to detail information. Then in the field of optics, it is believed that the detail information of samples cannot pass through conventional light microscopes. However, according to the results of this study, these opinions may need some revision, at least in the condition of isolated lighting. On the one hand, although diffraction-blurred images do not reflect details directly, they still carry the full information (including both profile and details) indirectly. On the other hand, it is possible to recover the ideal images (with details) from the observed images (comprising only low frequency components), without decreasing the samples' spatial frequency before imaging. In short, although the sample's high frequency components cannot pass through diffraction-limited microscopes, the detail information of the spatial structure could, using the prior knowledge of isolated lighting. So shall we conclude that the diffraction-limit is the limit for human eyes to resolve the details in the images from light microscope, but not for computers (machines) to extract super-resolution detail information?

The technique of image deconvolution is usually employed for the recovery of degraded images, e.g., relieving the effect of defocused light. In this study, the proposed methods are developed based on image deconvolution. They can extract sharp images from diffraction-blurred images, and get full details of samples' spatial structure, in certain condition (isolated lighting). Therefore, this technique could be named "Deconvolutional Super-resolution (DeSu-re)". It has the advantages of conventional microscopes, does not required decreasing the spatial frequency of samples', and could achieve unlimited resolution in principle. The simulation experiments directly prove 2~3 times of resolution improvement for the spatial method, and 2~5 times of improvement for the frequency method. In addition, they also indirectly prove 2~20 times of improvement for both methods. One of the future directions is to achieve higher resolution and verify the effectiveness in practice.

PeerJ Preprints | https://doi.org/10.7287/peerj.preprints.27591v1 | CC BY 4.0 Open Access | rec: 16 Mar 2019, publ: 16 Mar 2019

There are still some practical difficulties, especially the strong effect of the original images' distortion, e.g., noises on the results. Therefore, it is also an important future direction to get practical results as near to simulation results as possible. With the development of imaging devices and the improvement of signal-noise ratio, the accuracy of the methods would also improve accordingly.

The proposed technique could be used in combination of other techniques such as conventional microscope, confocal microscope, existing super-resolution methods, and so on. By extracting more details directly from the images of these techniques, higher resolution could be achieved. For example, some techniques have achieved very high resolution, and also provide conditions similar to isolated lighting. Combining with them, it is possible to further resolve the inner details of individual molecules, fluorescent probes or tiny light sources after localization.

Acknowledgements

We appreciate BPTC, BYSY, CNL, HDL, HL, LTU, LPU and LIBP for their support and resources.

References

1. Sigal, Y.M., R.B. Zhou, and X.W. Zhuang, *Visualizing and discovering cellular structures with super-resolution microscopy.* Science, 2018. **361**(6405): p. 880-887.
2. Hell, S.W. and J. Wichmann, *Breaking the diffraction resolution limit by stimulated emission: stimulated-emission-depletion fluorescence microscopy.* Optics Letters, 1994. **19**(11): p. 780-782.
3. Hofmann, M., et al., *Breaking the diffraction barrier in fluorescence microscopy at low light intensities by using reversibly photoswitchable proteins.* Proceedings of the National Academy of Sciences of the United States of America, 2005. **102**(49): p. 17565-17569.
4. Gustafsson, M.G., *Surpassing the lateral resolution limit by a factor of two using structured illumination microscopy.* J Microsc, 2000. **198**(Pt 2): p. 82-7.
5. Gustafsson, M.G.L., *Nonlinear structured-illumination microscopy: Wide-field fluorescence imaging with theoretically unlimited resolution.* Proceedings of the National Academy of Sciences of the United States of America, 2005. **102**(37): p. 13081-13086.
6. Rust, M.J., M. Bates, and X.W. Zhuang, *Sub-diffraction-limit imaging by stochastic optical reconstruction microscopy (STORM).* Nature Methods, 2006. **3**(10): p. 793-795.
7. Betzig, E., et al., *Imaging intracellular fluorescent proteins at nanometer resolution.* Science, 2006. **313**(5793): p. 1642-5.
8. Sharonov, A. and R.M. Hochstrasser, *Wide-field subdiffraction imaging by accumulated binding of diffusing probes.* Proceedings of the National Academy of Sciences of the United States of America, 2006. **103**(50): p. 18911-18916.
9. Balzarotti, F., et al., *Nanometer resolution imaging and tracking of fluorescent molecules with minimal photon fluxes.* Science, 2017. **355**(6325): p. 606-612.
10. Chen, F., P.W. Tillberg, and E.S. Boyden, *Expansion microscopy.* Science, 2015. **347**(6221): p. 543.
11. Gonzalez, R.C. and R.E. Woods, *Digital Image Processing (3rd Edition)*. 2014: PEARSON.
12. Moulin, P. and J.A.O. Sullivan, *Information-theoretic analysis of information hiding.* IEEE Transactions on Information Theory, 2003. **49**(3): p. 563-593.
13. Xie, Y., X. Tang, and M. Sun. *Image Compression Based on Classification Row by Row and LZW Encoding*. in *2008 Congress on Image and Signal Processing*. 2008.

14. Zitzmann, C., et al. *Hidden information detection based on quantized Laplacian distribution*. in *2012 IEEE International Conference on Acoustics, Speech and Signal Processing (ICASSP)*. 2012.
15. Lay, D.C., S.R. Lay, and J.J. McDonald, *Linear Algebra and Its Applications (5th Edition)*. 2015: PEARSON.
16. Oppenheim, A.V. and R.W. Schafer, *Digital Signal Processing*. 2015: PEARSON.

PeerJ Preprints | https://doi.org/10.7287/peerj.preprints.27591v1 | CC BY 4.0 Open Access | rec: 16 Mar 2019, publ: 16 Mar 2019